

# Phase Field Simulation of Thermotransport

---

*R R Mohanty, Y H Sohn*

Advanced Materials Processing and Analysis Center and  
Department of Mechanical, Materials and Aerospace Engineering  
University of Central Florida, Orlando FL

Collaboration with  
**Dr. Jonathan Guyer, NIST**



NIST Diffusion Workshop, May 12 & 13, 2008



# Outline

- ❖ **Overview of Our Research**
- ❖ **Introduction**
- ❖ **Motivation**
- ❖ **Mathematical Formulation**
- ❖ **Model Description**
- ❖ **Results**
- ❖ **Summary**
- ❖ **Future Work**

# Prime-Reliant Coatings for Gas Turbines

## Overview

Motivation

Introduction

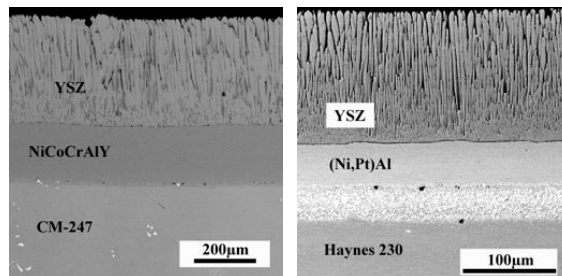
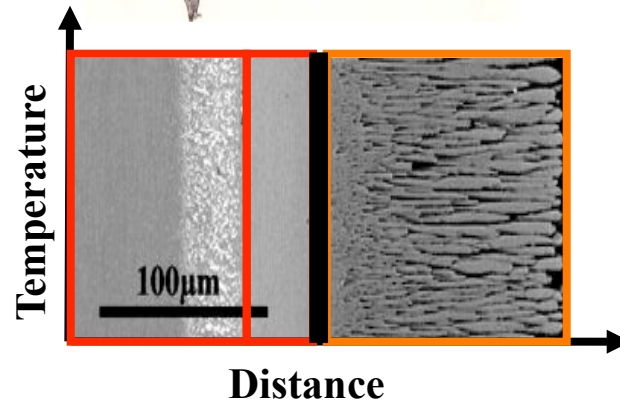
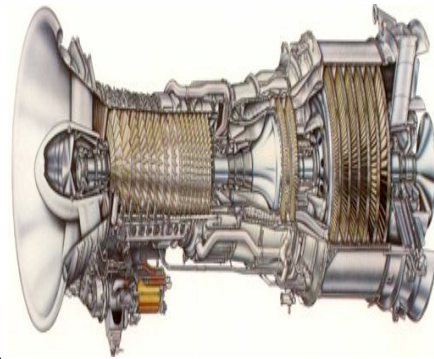
Formulation

The Model

Results

Summary

Future Work



**Topcoat:  $ZrO_2-8wt.\%Y_2O_3$**

$t' \rightarrow t \rightarrow (f+m)$  Phase Transformations  
Sintering, Microstructure and Strain Tolerance

**Thermally Grown Oxide (TGO)**

Thermal Expansion/Contraction Mismatch  
Transient/Initial Oxidation  
Phase Constituents ( $\alpha-Al_2O_3$  and Others) and Transformations

**Bond coat: (Ni,Pt)Al or NiCoCrAlY**

Phase Transformations and Constituents  
Inward and Outward Interdiffusion  
Creep Deformation/Surface Undulation

**Superalloy Substrates**

Phase Transformations and Constituents  
Outward Interdiffusion  
Creep Deformation



# Isothermal Coating-Substrate Diffusion

## Overview

Motivation

Introduction

Formulation

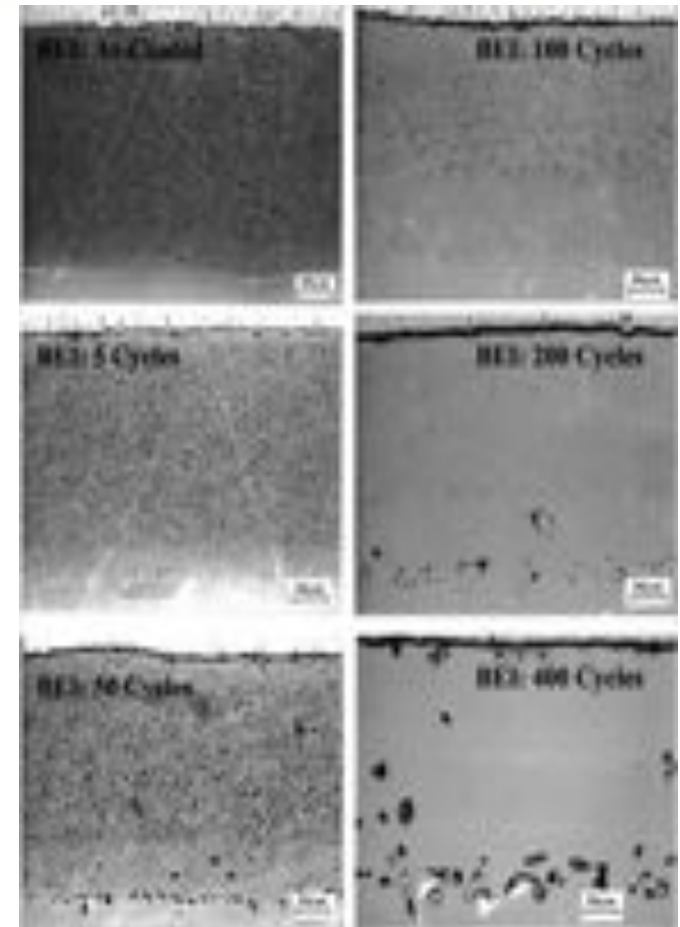
The Model

Results

Summary

Future Work

- ❖ Al Diffuses Out to Form  $\text{Al}_2\text{O}_3$  Scale.
  - Polymorphic Transformation of  $\text{Al}_2\text{O}_3$  Scale.
- ❖ Al Diffuses into the Substrate:
  - Dissolution of High Al  $\beta$  phase.
  - Formation of Oxide Scale Rich in Ni, Co and Cr.
  - Formation of Kirkendall Porosity.
- ❖ Elements Added to Substrate for High-Temperature Strengthening Diffuse into the Coating:
  - Affect Near-Surface Mechanical Properties of a Component.
  - Affect the Formation or Adherence of the Protective Oxide Scale.



Backscatter electron micrographs of NiCoCrAlY-IN738 illustrating dissolution of  $\beta$ -phase as a function of thermal cyclic oxidation at  $1121^\circ\text{C}$

# Isothermal PFM

## $\gamma$ vs. $\gamma+\gamma'$ Diffusion Couples in Ni-Al Alloys

### Overview

Motivation

Introduction

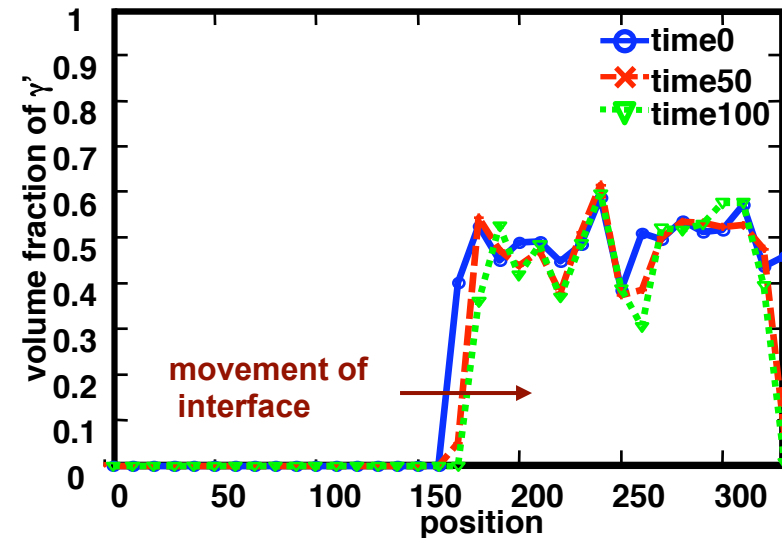
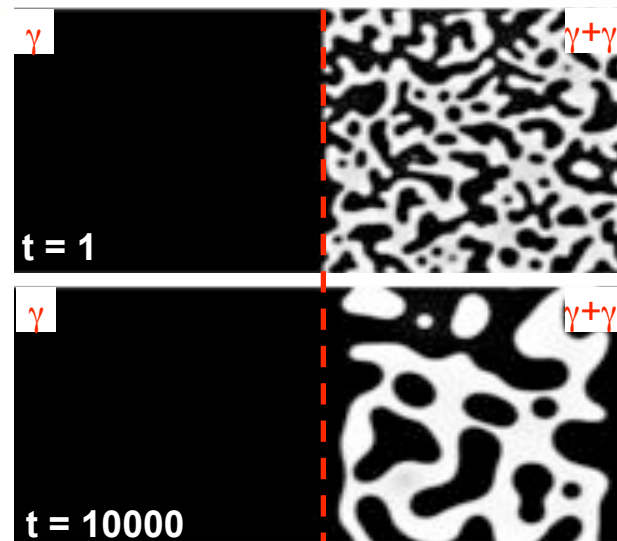
Formulation

The Model

Results

Summary

Future Work



### Simulated microstructure and volume fraction profile of $\gamma$ vs. $\gamma+\gamma'$ couple.<sup>1</sup>

- ❖ Boundary Movement towards two-phase region:  $\gamma > \gamma+\gamma'$
- ❖ Addition of  $\gamma$  phase at the boundary: type I boundary.
- ❖ Depletion of  $\gamma+\gamma'$  region or increase in  $\gamma$  phase region was observed experimentally by Susan et al.<sup>2</sup>

<sup>1</sup>R. R. Mohanty, A. Leon and Y. H. Sohn, *Comp. Mater. Sci*, in Press, 2008.

<sup>2</sup>D. F. Susan and A. R. Marder, *Acta Mater.* 49, 2001, 1153.

# $\gamma$ vs. $\gamma+\beta$ (Ni-Cr-Al) Diffusion Couples Composition-Dependent Microstructural Evolution

## Overview

Motivation

Introduction

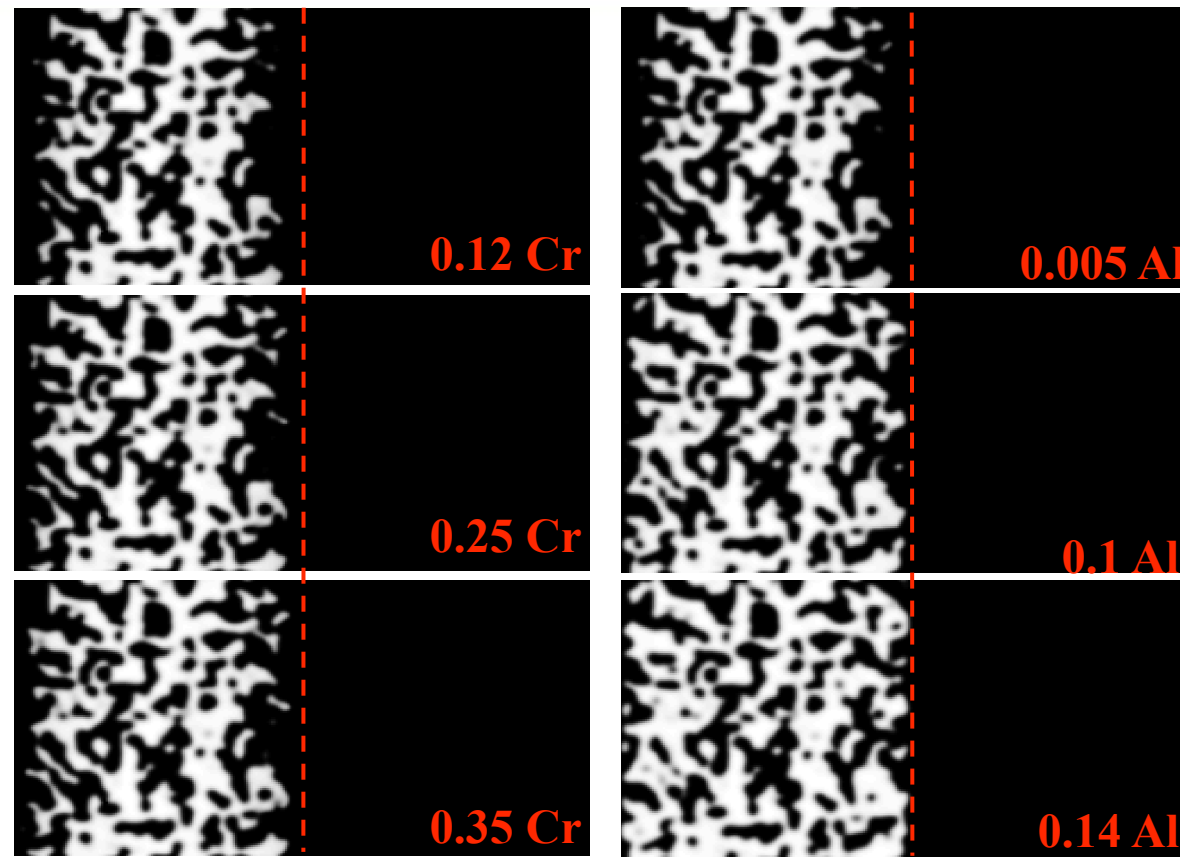
Formulation

The Model

Results

Summary

Future Work



**Higher concentration of Cr and Al yields lower dissolution rate of  $\beta$  phase and slower movement of the  $\gamma/\gamma+\beta$  boundary.**



# $\gamma$ vs. $\gamma+\beta$ (Ni-Cr-Al) Diffusion Couples Composition-Dependent Microstructural Evolution

## Overview

Motivation

Introduction

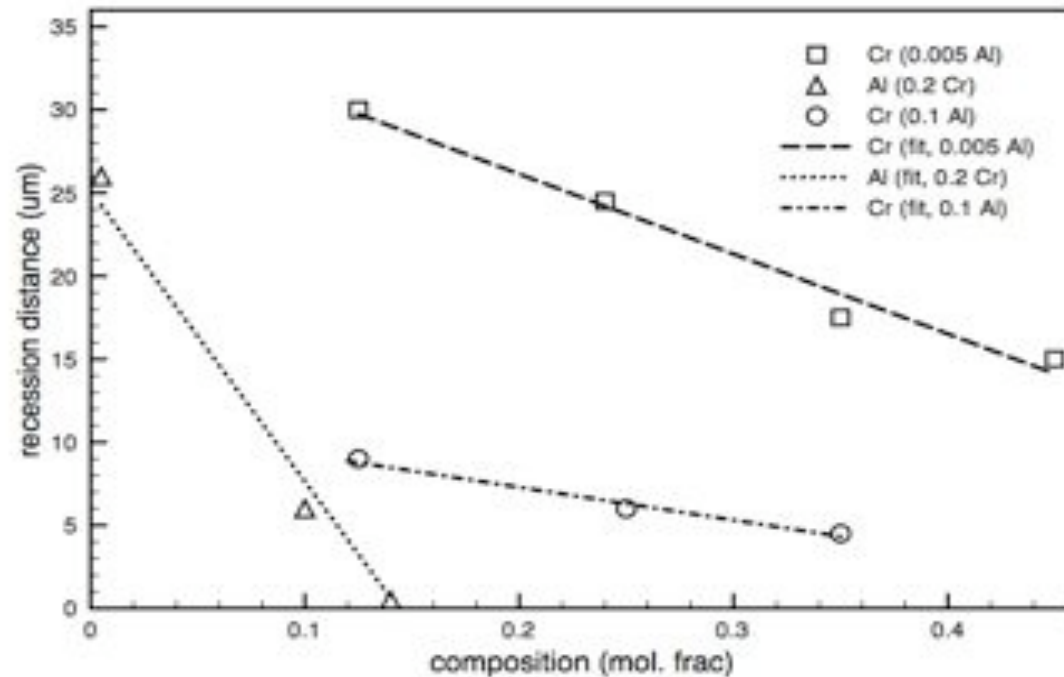
Formulation

The Model

Results

Summary

Future Work



**Recession Distance of  $\gamma+\beta$  region vs. Al and Cr concentration in the single phase  $\gamma$  alloy as predicted by phase field simulation.**

Concentration of Al has greater effect on the dissolution of  $\beta$  phase and movement of the  $\gamma/\gamma+\beta$  interface.

# $\gamma$ vs. $\gamma+\beta$ (Ni-Cr-Al) Diffusion Couples Concentration Profiles

## Overview

Motivation

Introduction

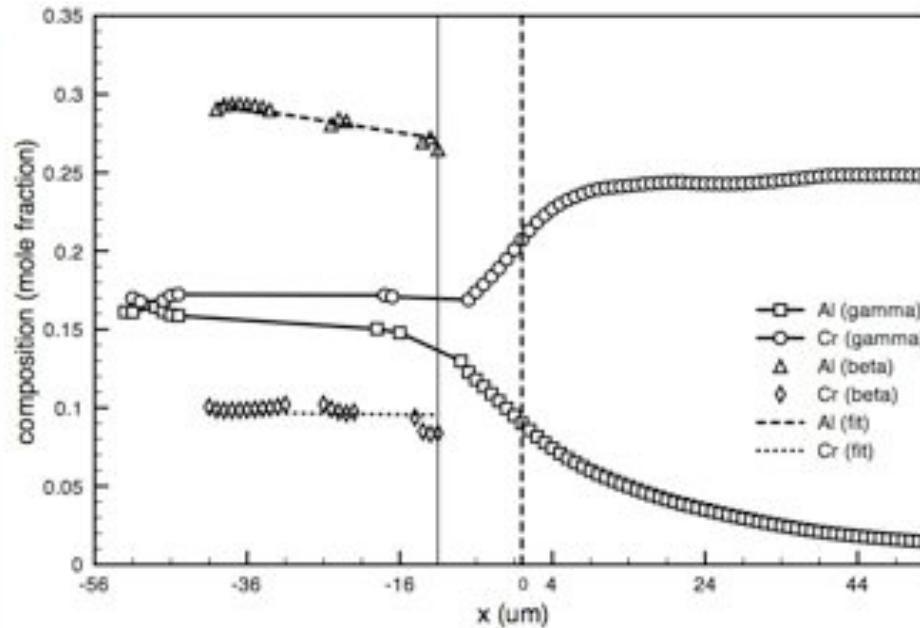
Formulation

The Model

Results

Summary

Future Work



Simulated composition profiles for the  $\gamma+\beta$ / $\gamma$  diffusion couple. The dashed and solid vertical lines are the location of the interface at  $t = 0$  and  $t = 2.5$  hour respectively.

- ❖ Interdiffusion occurs both in the  $\gamma$  and  $\gamma+\beta$  regions (i.e., limitation of a typical sharp interface models).
- ❖ Concentrations of  $\gamma$  and  $\beta$  phases in the  $\gamma+\beta$  region are close to the equilibrium compositions.

# Motivation for The Present Work

Overview

Motivation

Introduction

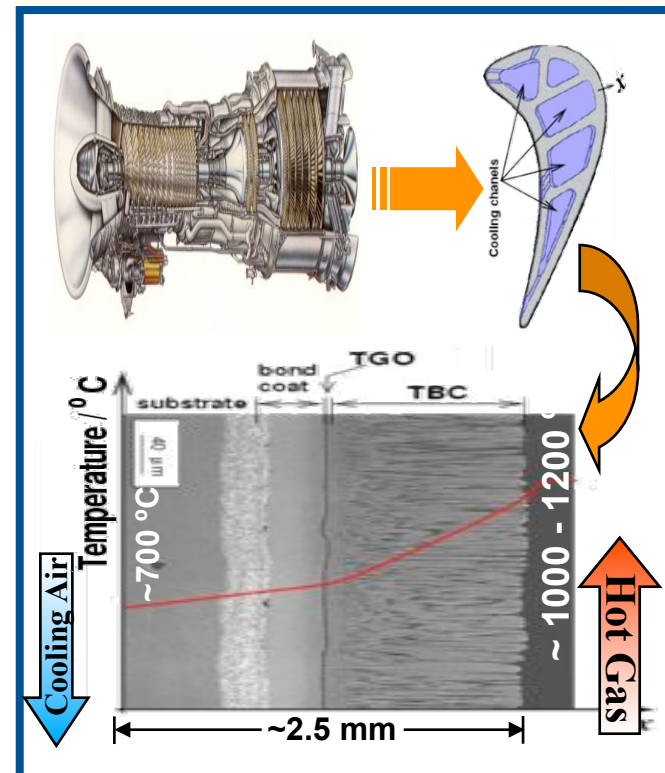
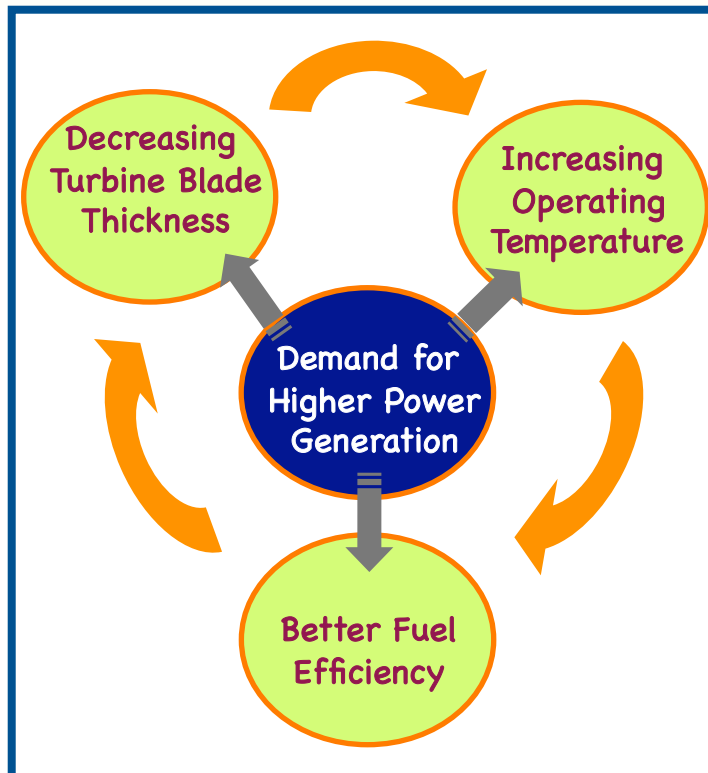
Formulation

The Model

Results

Summary

Future Work



- ❖ Decreasing Thickness of Turbine Blades, Increasing Miniaturization in Electronics Industry
- ❖ Demand for More MW, Increasing Operating Temperatures and Better Efficiency in Nuclear Energy Production

# Motivation for The Present Work

Overview

Motivation

Introduction

Formulation

The Model

Results

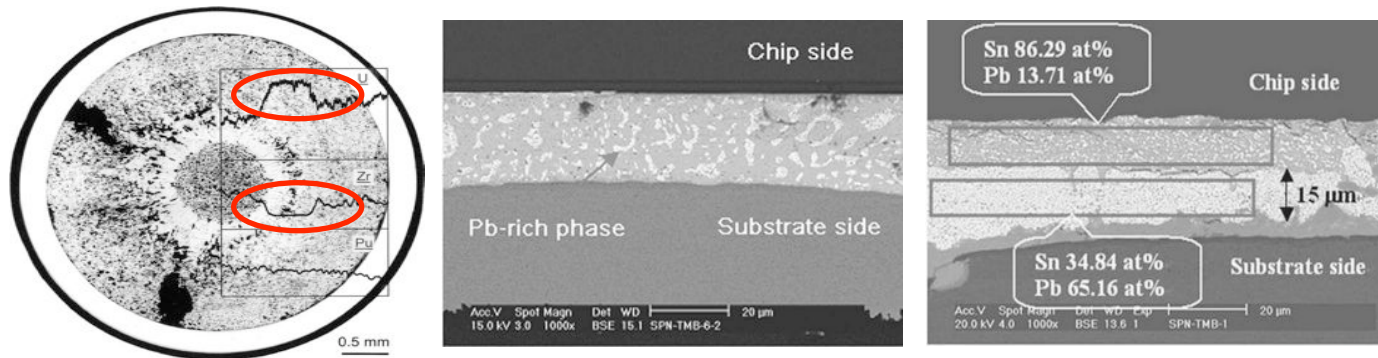
Summary

Future Work

- ❖ Large magnitude of temperature gradient can exist:

Turbine Blades  $\approx 120 - 200 \text{ }^\circ\text{C/mm}$

Nuclear Fuel  $\approx 240 \text{ }^\circ\text{C/cm}$



## Composition and Phase Redistribution in Nuclear Fuel and Chip Interconnects

- ❖ Constituent and Phase Redistribution due to temperature gradient:
  - Change in Solidus Temperature  $\rightarrow$  unwanted melting
  - Causes phase transformations
  - Change in physical and mechanical properties

# Motivation for The Present Work

Overview

Motivation

Introduction

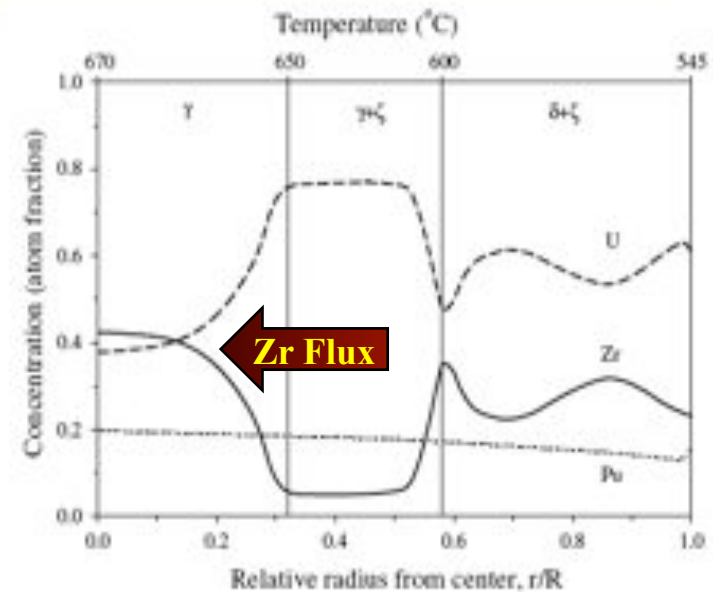
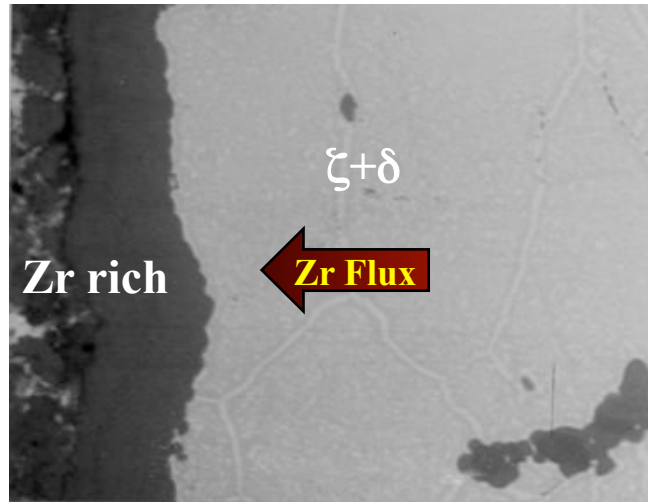
Formulation

The Model

Results

Summary

Future Work



## Composition and Phase Redistribution in U-Pu-Zr Nuclear Fuel

- ❖ Constituent redistribution in U-Pu-Zr alloy<sup>1,2</sup>:
  - Phase transformation occurred from the initial  $\gamma$ -bcc phase upon thermotransport treatment.
  - Zr flux towards the hot end forming a Zr rich layer.

<sup>1</sup>Y.H.Sohn, M.A.Dayananda, G.L.Hofman, R.V.Strain, S.L.Hayes, *J. Nuclear Mater.* (2000), 279, 317.

<sup>2</sup>Y. Kim, G. Hofman, S. Hayes and Y. H. Sohn, *J. Nuclear Mater.* (2004), 327, 27.

# The Thermotransport Phenomenon

Overview

Motivation

Introduction

Formulation

The Model

Results

Summary

Future Work

- ❖ Development of concentration gradient in a homogeneous alloy when a temperature gradient is applied - Ludwig - Soret effect.

- ❖ Fick's 1st Law must be modified to account for the effect of temperature gradient on the diffusion flux:

$$J_i = -D_i \frac{\partial c_i}{\partial x} - D'_i c_i \frac{\partial T}{\partial x}$$

where,  $D_i$  and  $D'_i$  are the isothermal and thermal diffusion coefficients<sup>1</sup>.

- ❖ The concentration gradient can eventually reach steady state.

$$J_i = 0 \Rightarrow -D_i \frac{\partial c_i}{\partial x} = D'_i c_i \frac{\partial T}{\partial x}$$

- ❖ The concentration gradient is a characteristic of the system.



# The Thermotransport Phenomenon

Overview

Motivation

Introduction

Formulation

The Model

Results

Summary

Future Work

- ❖ For an interstitial solute in a binary alloy, the flux equation relative to lattice can be written as:

$$J = -\frac{Dc}{RT} \left[ RT \frac{d \ln c}{dx} + \frac{Q^*}{T} \frac{dT}{dx} \right]$$

where,  $Q^*$  = amount of heat carried per atom (Heat of Transport)

Steady state distribution is defined by only one  $Q^*$

- ❖ For a substitutional alloy, relative rate of movement of solute and solvent are important:

$$J_i = -\frac{D_i c_i}{RT} \left[ RT \frac{d \ln c_i}{dx} + \frac{Q_i^*}{T} \frac{dT}{dx} \right]$$

where,  $i$  denotes each element.

Condition for Validity: Vacancy mechanism of diffusion  
Equilibrium vacancy concentration

Diffusivity and  $Q^*$  for both the elements necessary.



# Formulation

Overview

Motivation

Introduction

Formulation

The Model

Results

Summary

Future Work

Constant Molar Volume and Density:  $V_m, \rho$

Concentration:  $n_i$  Mole Fraction:  $c_i$

Mass Balance:  $\sum_i n_i = \rho = \frac{1}{V_m}, \sum_i c_i = 1.0$

**Model System**

Binary Substitutional Alloy:

components A, B

- ❖ Vacancy mechanism for diffusion
- ❖ Vacancies exist everywhere in equilibrium concentration under the thermal gradient<sup>1</sup>



# Formulation

Overview

Motivation

Introduction

Formulation

The Model

Results

Summary

Future Work

## Lattice Frame of Reference

- ❖ From the Onsager's linear relationship of fluxes and forces, the flux equation under thermal gradient is<sup>1</sup>:

$$J_k = \sum_{i=1}^{n-1} L_{ki} (X_i - X_n + Q_i^* X_q) \quad [1]$$

where,

$$X_i = -\nabla\mu_i : \text{Chemical Driving Force}$$

$$X_q = -\frac{\nabla T}{T} : \text{Thermal Driving Force}$$

$$Q_i^* : \text{Heat of Transport}$$

- ❖ With the vacancy mechanism for diffusion being operative, vacancy ( $v$ ) is treated as the third constituent<sup>2</sup>, so that;

$$J_A = L_{AA} (X_A - X_v + Q_A^* X_q) + L_{AB} (X_B - X_v + Q_B^* X_q) \quad [2a]$$

$$J_B = L_{BA} (X_A - X_v + Q_A^* X_q) + L_{BB} (X_B - X_v + Q_B^* X_q) \quad [2b]$$

where,  $L_{ij}$  are Onsager's phenomenological coefficients.

1. De Groot S. R., "Thermodynamics of Irreversible Processes", 1952

2. Howard R. E. and Lidiard A. B., "Matter Transport in Solids", Rep. Prog. Phys., 27, p.161.

# Formulation

Overview

Motivation

Introduction

Formulation

The Model

Results

Summary

Future Work

- ❖ Assuming vacancies exist everywhere in their equilibrium concentration in a dilute solution<sup>1</sup>:

$$X_v = -\nabla\mu_v = -kT \frac{\nabla c_v}{c_v} = -h_{fv} \frac{\nabla T}{T} = h_{fv} X_q \quad [3]$$

where,  $h_{fv}$  is the **enthalpy of formation of a vacancy**.

- ❖ Substituting this in the flux equation:

$$J_A = L_{AA} \left[ X_A + (Q_A^* - h_{fv}) X_q \right] + L_{AB} \left[ X_B + (Q_B^* - h_{fv}) X_q \right] \quad [4a]$$

$$J_B = L_{BA} \left[ X_A + (Q_A^* - h_{fv}) X_q \right] + L_{BB} \left[ X_B + (Q_B^* - h_{fv}) X_q \right] \quad [4b]$$

- ❖ Since :  $c_v \ll c_A, c_B$  , applying Gibbs-Duhem relation:

$$c_A X_A + c_B X_B + c_v X_v \approx c_A X_A + c_B X_B \approx 0 \quad [5]$$



# Formulation

Overview

Motivation

Introduction

Formulation

The Model

Results

Summary

Future Work

- ❖ Using law of mass conservation in Eq.(5) we can write:

$$L_{AA} X_A + L_{AB} X_B = \frac{cL_{AA} - (1-c)L_{AB}}{c} X_A = \rho(1-c)\beta_A X_A \quad [6a]$$

$$L_{BB} X_B + L_{BA} X_A = \frac{(1-c)L_{BB} - cL_{BA}}{1-c} X_B = \rho c \beta_B X_B \quad [6b]$$

where,  $\beta_i$  corresponds to atomic mobilities of individual elements and  $c$  is the mole fraction of B.

- ❖ Substituting Eq. 6 in the flux equation (Eq.4) :

$$J_A = -\rho(1-c)\beta_A \nabla \mu_A + \left[ L_{AA} (Q_A^* - h_{fv}) + L_{AB} (Q_B^* - h_{fv}) \right] X_q \quad [7a]$$

$$J_B = -\rho c \beta_B \nabla \mu_B + \left[ L_{BA} (Q_A^* - h_{fv}) + L_{BB} (Q_B^* - h_{fv}) \right] X_q \quad [7b]$$

# Formulation

Overview

Motivation

Introduction

Formulation

The Model

Results

Summary

Future Work

## Laboratory Frame of Reference

- ❖ In the laboratory frame of reference sum of the fluxes vanishes:

$$\tilde{J}_A + \tilde{J}_B = 0 \quad [8a]$$

$$\text{or, } \tilde{J}_A = -\tilde{J}_B = J_A - (1-c)(J_A + J_B) = cJ_A - (1-c)J_B \quad [8a]$$

- ❖ Substituting the intrinsic fluxes from Eq. 7 and using Onsager's reciprocal relation,  $L_{ij} = L_{ji}$ :

$$\begin{aligned} \tilde{J}_A &= -\rho c(1-c)\beta_A \nabla \mu_A + \rho c(1-c)\beta_B \nabla \mu_B + \\ & [cL_{AA} - (1-c)L_{BA}]Q_A^{*'} X_q + [cL_{AB} - (1-c)L_{BB}]Q_B^{*'} X_q \quad [9] \\ &= -\rho c(1-c)[\beta_A \nabla \mu_A - \beta_B \nabla \mu_B] + \rho c(1-c) \left[ \beta_A Q_A^{*'} - \beta_B Q_B^{*'} \right] X_q \end{aligned}$$

where,  $Q_i^{*'} = Q_i^* - h_{fv}$

# Formulation

Overview

Motivation

Introduction

Formulation

The Model

Results

Summary

Future Work

- ❖ Applying Gibbs-Duhem relation:

$$\nabla\mu_A = c\nabla\mu_A^{eff}, \nabla\mu_B = -(1-c)\nabla\mu_A^{eff} \quad [10]$$

$$\text{where, } \nabla\mu_A^{eff} = -\nabla\mu_B^{eff} = \nabla(\mu_A - \mu_B) \quad [11]$$

- ❖ Substituting Eq. 11 in the flux equation, Eq. 9, the final flux equation can be written as :

$$\begin{aligned} \tilde{J}_A &= -\rho c(1-c)[c\beta_A + (1-c)\beta_B]\nabla\mu_A^{eff} + \rho c(1-c)\left[\beta_A Q_A^{*'} - \beta_B Q_B^{*'}\right]X_q \\ &= -M_c \nabla\mu_A^{eff} + M_Q X_q \end{aligned} \quad [12a]$$

$$\tilde{J}_B = -\tilde{J}_A = -M_c \nabla\mu_B^{eff} + M_Q \frac{\nabla T}{T} \quad [12b]$$

$$M_c = \rho c(1-c)[c\beta_A + (1-c)\beta_B]$$

$$M_Q = \rho c(1-c)\left[\beta_A Q_A^{*'} - \beta_B Q_B^{*'}\right]$$

# The Model

Overview

Motivation

Introduction

Formulation

The Model

Results

Summary

Future Work

- ❖ A simple regular solution model was used for the chemical free energy of the system :

$$f(c,T) = RT \left[ c \ln c + (1-c) \ln(1-c) \right] + \chi c(1-c)$$

- ❖ The Cahn-Hilliard free energy functional is defined as:

$$F = N_V \int_V \left[ f(c,T) + \kappa (\nabla c)^2 \right] dV$$

where,  $N_V$  is the total number of atoms in the system,  $V$  is the volume and  $\kappa$  corresponds to gradient energy coefficients.

- ❖ In an inhomogeneous system the effective chemical potential can be obtained as:

$$\mu_B^{eff} = \frac{\delta F}{\delta n_B} = V_m \frac{\delta F}{\delta c}$$

# The Model

Overview

Motivation

Introduction

Formulation

The Model

Results

Summary

Future Work

- ❖ Now the flux equation can be written as:

$$\tilde{J}_B = -V_m M_c \nabla \left( \frac{\partial f}{\partial c} - 2\kappa_c \nabla^2 c \right) + M_Q \frac{\nabla T}{T}$$

- ❖ The spatio-temporal evolution of composition is governed by the continuity equation:

$$\begin{aligned} \frac{\partial n_B}{\partial t} &= \frac{1}{V_m} \frac{\partial c(x,t)}{\partial t} = -\nabla \cdot \tilde{J}_B \\ &= \nabla \cdot \left[ V_m M_c \nabla \left( \frac{\partial f}{\partial c} - 2\kappa_c \nabla^2 c \right) - M_Q \frac{\nabla T}{T} \right] \end{aligned}$$

- ❖ Applied to both single phase and two phase alloys of a binary system.

# Numerical Implementation

Overview

Motivation

Introduction

Formulation

The Model

Results

Summary

Future Work

- ❖ The governing equation was made dimensionless for numerical convenience.
- ❖ Both constant and functions of temperature was used for atomic mobility and heat of transport values.
- ❖ Numerical calculations were performed using Fipy Partial Differential Equation (PDE) solver using a finite volume approach.
- ❖ Simulations of single phase (1D) and two phase (2D) were performed.

$$\beta_i = A_i \exp\left(-Q_i/RT\right) \quad (\text{Arrhenius}^1)$$

$$Q_i^* = B_i + C_i T \quad (\text{Linear}^2)$$



# Temperature Distribution and Free Energy

Overview

Motivation

Introduction

Formulation

The Model

Results

Summary

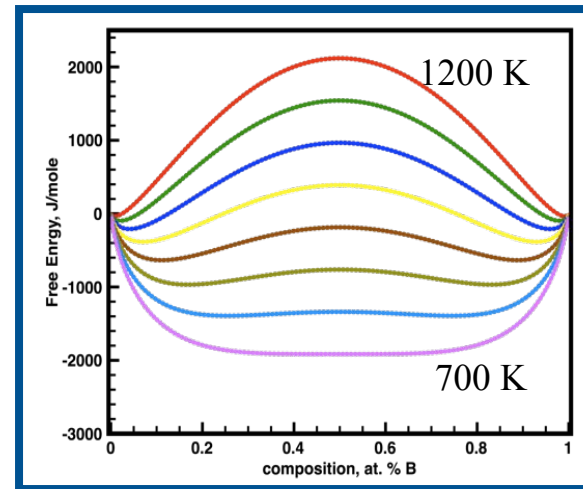
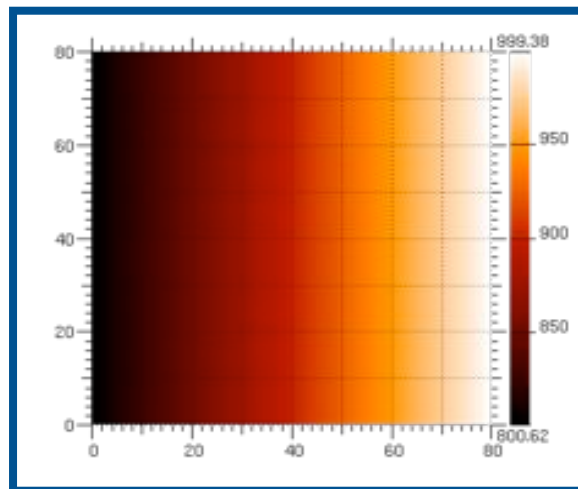
Future Work

- ❖ The temperature field obeys Laplace's equation

$$\nabla^2 T = 0$$

subjected to boundary conditions

$$J_q \cdot \hat{n} = 0, T|_{x=0} = T_{\min}, T|_{x=L} = T_{\max}$$



**Applied temperature gradient and the free energy vs. composition curves at different temperatures.**

# Results

## 1D Simulation of Single Phase Alloy

Overview

Motivation

Introduction

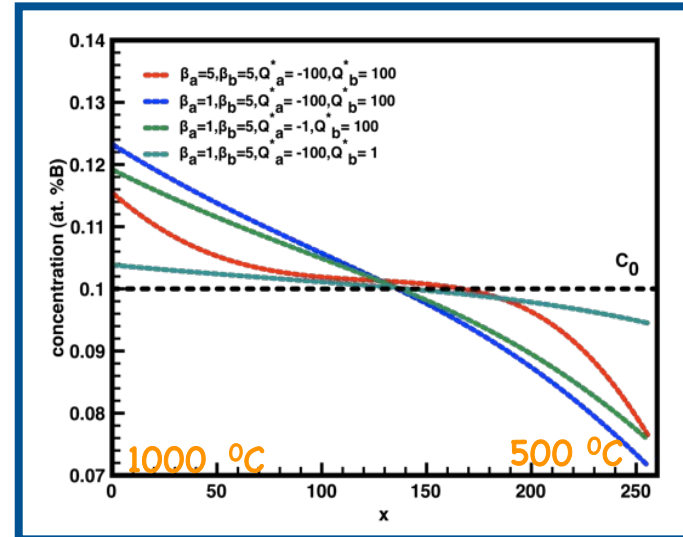
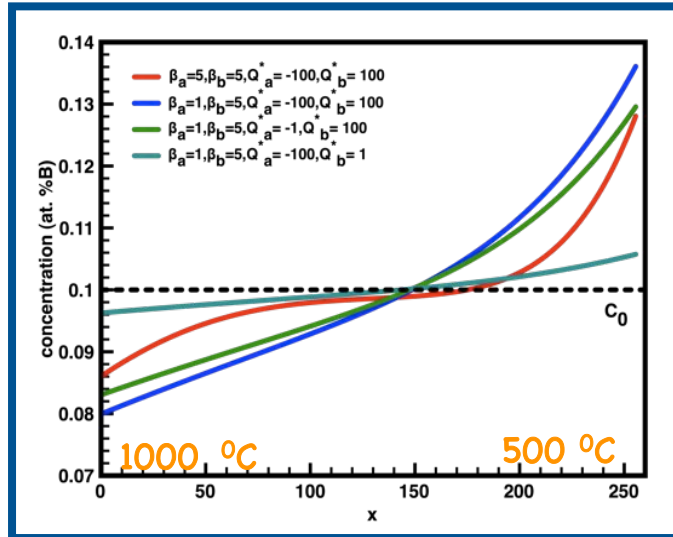
Formulation

The Model

Results

Summary

Future Work



**Composition Profiles of Component B developed under Temperature Gradient for various combinations of  $\beta$  and  $Q^*$ .**

- ❖ The concentration gradient depends on the initial composition and the values of atomic mobility as well as heat of transport.
- ❖ Steady state can be reached after a long time of anneal under thermal gradient.

# Results

## 2D Simulation of Two Phase Alloy

Overview

Motivation

Introduction

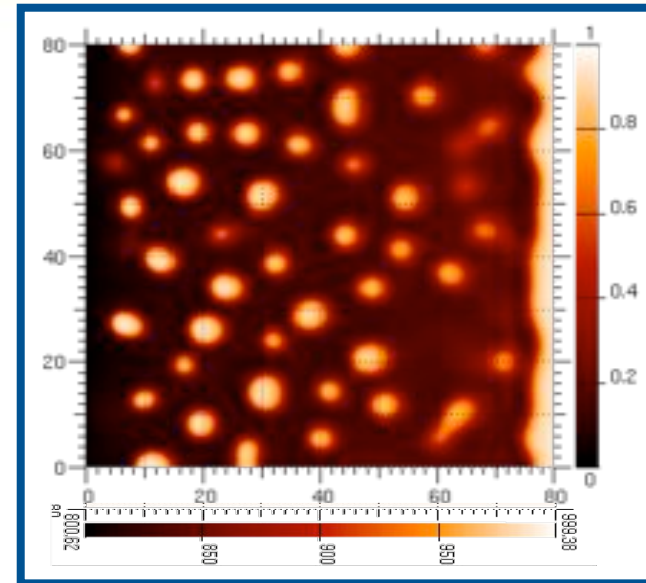
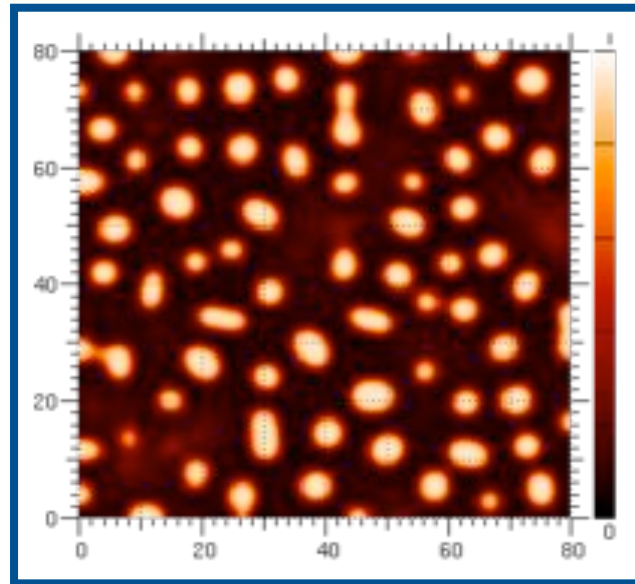
Formulation

The Model

Results

Summary

Future Work



**Phase distribution before and after the application of temperature gradient. The bright regions are B rich phase.**

- ❖ Preferential movement of B atoms towards the hot end and A atoms towards the cold end.
- ❖ Phase redistribution occurs with B rich and A rich single phase regions forming at the hot and cold ends.

# Results

## 2D Simulation of Two Phase Alloy

Overview

Motivation

Introduction

Formulation

The Model

Results

Summary

Future Work

- ❖ Elements in a substitutional alloy can have similar mobilities.
- ❖  $\beta$  and  $Q^*$  values of all the elements are important and needs to be considered.
- ❖ Combination of  $\beta$  and  $Q^*$  decide the magnitude and sign of  $M_Q$
- ❖ Four cases were considered:

Case - I:  $Q_A^* = Q_B^*$  and  $M_Q < 0$

Case - II:  $Q_B^* \gg Q_A^*$  and  $M_Q < 0$ ,  $|M_Q|$  is large

Case - III:  $Q_B^* \ll Q_A^*$  and  $M_Q > 0$ ,  $|M_Q|$  is large

Case - IV:  $Q_B^* < Q_A^*$  and  $M_Q > 0$ ,  $|M_Q| \approx 0$

In all the four cases  $\beta_B > \beta_A$  and  $Q_A^*, Q_B^* > 0$ .

# 2D Simulation of Two Phase Alloy

Overview

Motivation

Introduction

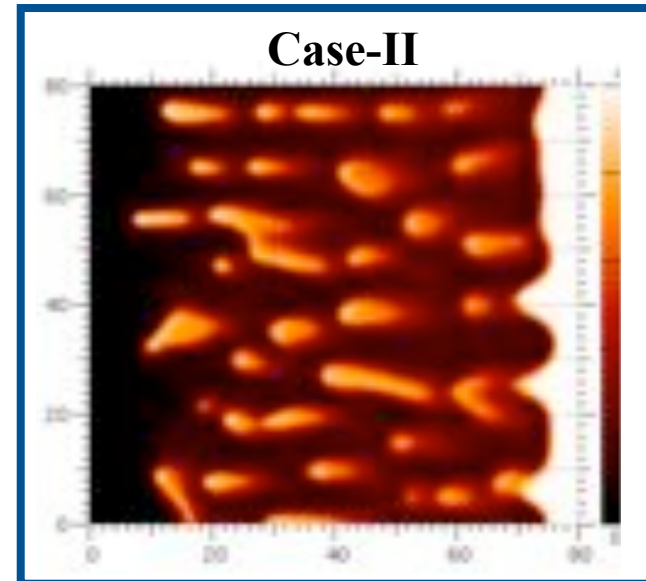
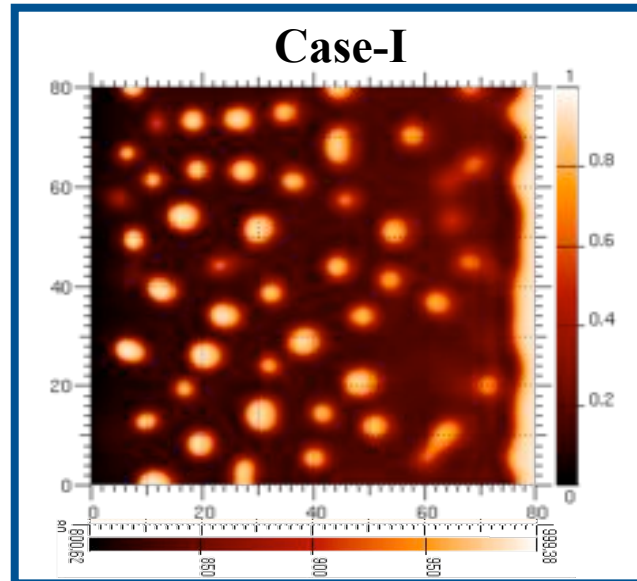
Formulation

The Model

Results

Summary

Future Work



**Phase distribution in a two phase alloy with different  $M_Q$  values subjected to temperature gradient.**

- ❖ Both in Case - I and Case - II,  $M_Q < 0$  and the contribution of temperature gradient to the flux is in the same direction to that of the concentration gradient.
- ❖ Stronger effect is evident in Case - II with a large  $M_Q$ .

# 2D Simulation of Two Phase Alloy

Overview

Motivation

Introduction

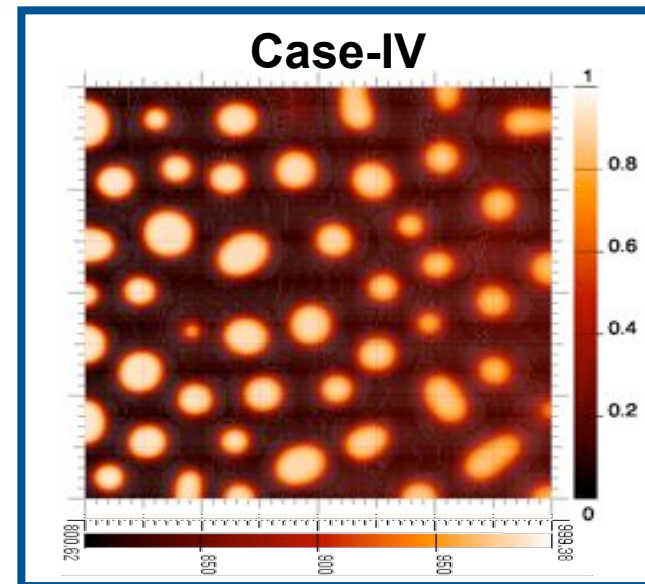
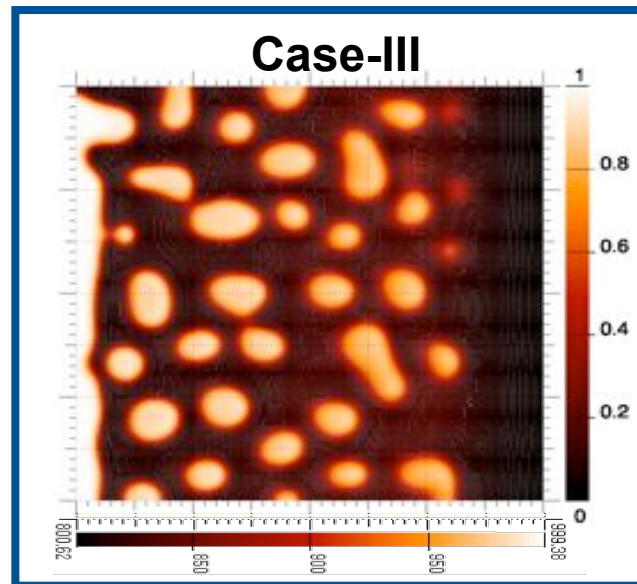
Formulation

The Model

Results

Summary

Future Work



**Phase distribution in a two phase alloy with different  $M_Q$  values subjected to temperature gradient.**

- ❖ Both in Case - III and Case - IV,  $M_Q > 0$  and the contribution of temperature gradient to the flux is in the opposite direction to that of the concentration gradient.
- ❖ Effect is negligible in Case - IV with  $M_Q \approx 0$ .

# Summary

Overview

Motivation

Introduction

Formulation

The Model

Results

Summary

Future Work

- ❖ A phase field model was devised to simulate Thermotransport phenomenon in binary alloys.
- ❖ Constituent and phase redistribution in single and two phase alloys were studied utilizing the model.
  - Concentration gradient developed in an initially homogeneous single phase alloy when subjected to temperature gradient.
  - A and B rich layer formed due to the preferential movement of atoms towards the hot or cold end.
  - The redistribution is dependent on the sign and magnitude of heat of transport and values of atomic mobilities.
- ❖ The model can use real thermodynamic and kinetic data.

# Future Work

Overview

Motivation

Introduction

Formulation

The Model

Results

Summary

Future Work

- ❖ Extension of the model to simulate real alloy systems using thermodynamic and kinetic database.
- ❖ Extension of the model to study ternary systems.

## *Acknowledgements*

Dr. Jonathan Guyer, NIST

Fipy Development Group, NIST